

Low Cost Modified Biochars from Peanut Shells for the Removal of Textile Dyes

Nelson Nunes,¹ Maria Teresa Santos^a and Angela Martins^{a,b}

^aDepartamento de Engenharia Química, Instituto Superior de Engenharia de Lisboa, Instituto Politécnico de Lisboa, R. Conselheiro Emídio Navarro, 1959-007 Lisboa, Portugal

^bCentro de Química Estrutural, Institute of Molecular Sciences, Faculdade de Ciências, Universidade de Lisboa, Campo Grande, 1749-016 Lisboa, Portugal

Biochars from peanut shell wastes were produced and further modified with KOH and HNO₃ to efficiently remove two industrial dyes, Mordant Orange 1 and Green Malachite oxalate, in aqueous systems. The materials were characterized through elemental analysis, N₂ adsorption isotherms, Fourier transform infrared (FTIR) spectroscopy, scanning electron microscopy (SEM), and the determination of the point of zero charge, pH_{PZC}. The basic and, particularly, the acid treatments increased the specific surface area by 15 and 43%, respectively, and the pH_{PZC} shifted from 6.2 to 9.1 or 3.3 upon treatments with KOH or HNO₃. These modifications impacted the adsorption behavior of the dyes; in the case of Mordant Orange 1, the adsorption capacity increased 2 and 4 times, respectively, when compared with the parent biochar. These results show that the performance of biochars can improve substantially through simple modifications using acid or basic treatments that not only increase the specific surface area but also modify adsorbent/adsorbate interactions.

Keywords: alkali or acid treatment, biochars, peanut shells, pyrolysis, dye adsorption

Introduction

Waste recycling is a key factor in a circular economy. Since municipal solid waste is composed mainly of food waste, the idea of using them as environmental decontamination agents is a concept of growing interest. Simultaneously, the contamination of aquatic environments by dyes is a problem that continues to be present in public discussion, especially when the source is the textile industry. In fact, during the last decades, dyes production has increased steadily, with more than 100,000 dyes being commercially available.^{1,2} Although wastewater from dyeing processes tends to have dyes in moderate concentrations, their intensive use can cause different environmental problems since these substances are stable and can accumulate in the surrounding environment, leading to toxic and carcinogenic effects.^{3,4} One of the classic methods to remove colored compounds from industrial wastewater is the use of adsorbent materials, being activated carbon the most used. Activated carbons are excellent adsorbents due to their high porosity and rich surface chemical composition, i.e., oxygen surface groups.⁵

However, the high energy costs involved in the production of activated carbons led to the search for alternative low-cost carbon-based adsorbent materials. Biochars are an alternative whose potentialities are currently being explored.

Biochar is defined as a carbon-rich solid product from the thermal pyrolysis of biomass and characterized by a large specific surface area and the presence of surface functional groups.^{6,7} The low costs involved in the production of these materials, as well as the abundant feedstocks, mainly wastes from food industry and agriculture, make the use of biochars very appealing. Several sources of biomass have been transformed into biochars, such as rice husk, coconut, walnut and groundnut shells, pinewood or raw fish scales, only to mention a few examples recently reviewed.^{8,9} Their adsorption properties have been tested for the removal of dyes,⁹⁻¹³ pharmaceuticals,^{8,14,15} antibiotics,⁷ NH₃-N,¹⁶ and heavy metals,^{17,18} among others.

The adsorption efficiency of biochars depends on multiple aspects related not only to the carbon source but also to the methodology used in the production method.⁵

The samples pre-processing, including washing steps, drying and sifting, proved to be of extreme importance along with the vital carbonization step, having a direct impact on the adsorption capacity of the materials. In fact, materials

*e-mail: nnunes@deq.isel.ipl.pt

Editor handled this article: Jafsa Fernandes Soares

treated with more severe conditions, that is, 800 °C, usually present the highest adsorption capacity.^{12,19} However, it must be emphasized the high energetic cost involved in the preparation of such adsorbent materials, especially when considering large scale production. Post-synthesis treatments are also applied aiming to modify texture and surface chemistry and, thus, increase the adsorption capacity of biochars, which can be interesting to improve the properties of materials, especially when prepared under mild carbonization temperatures.⁷ Alkali and acid treatments are attractive modification methods due to their low cost, good effectiveness and easy implementation, even at a large scale. For instance, it was already demonstrated that alkali treatments with KOH have a positive influence on the adsorption capacity of biochars in the presence of metal cations, anions,²⁰ and organic compounds.¹⁴ Acid treatments are also mentioned in the literature, using HNO₃,²¹ H₂SO₄,^{22,23} or H₃PO₄,^{23,24} but are less explored when compared with alkaline treatments. These activation methods work according to different mechanisms, one of the most important is the increase of surface functional groups, namely hydroxyl and carbonyl, adding to the ones already present in biochars. The additional groups increase possible electrostatic interactions and hydrogen bonding leading to higher adsorption capacities. These treatments also modify the morphology and pore structure of the biochars, resulting in different outcomes (depending on the agent and mode of treatment used), with some increasing the surface area while others reduce it.²¹

The purpose of this work was to obtain effective biochar-based adsorbents in the removal of dyes from textile industries, using peanut shells as raw material. The experimental conditions selected to produce the biochar samples were chosen to minimize the production costs using optimized mild pyrolysis conditions. To improve the adsorbent properties and based on the assumptions of chemical activation mentioned before, the materials were submitted to a post-synthesis alkali or acid treatment using KOH or HNO₃ solutions. The adsorption capacities of biochar materials were studied using two commercial textile dyes whose molecular structures are presented in Figure 1.

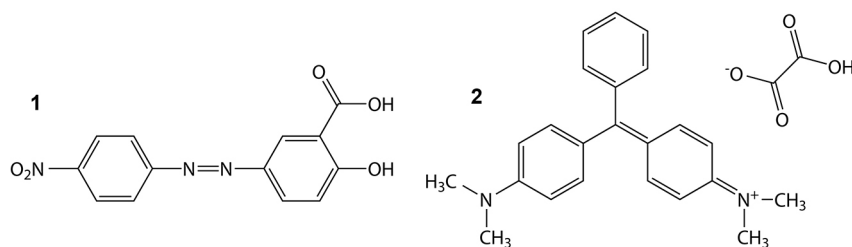


Figure 1. Used dyes. (1) Mordant Orange 1, molecular weight (Mw) = 287.23 g mol⁻¹, pK_a = 11.2 and (2) Green Malachite oxalate, Mw = 463.50 g mol⁻¹, pK_{a1} = 6.9, pK_{a2} = 10.3.

Mordant Orange 1 (herein designated as MO-1) belongs to the category of azo dyes due to the presence of one or more azo bonds (-N=N-) and aromatic rings and is very stable in the natural environment. As most azo dyes, MO-1 is used for coloring many different materials such as textiles, leather, plastics, food, and pharmaceuticals. Green Malachite oxalate salt (herein designated as GM) is a *N*-methylated diaminotriphenylmethane dye used not only as a textile dye but also as a fungicide and ectoparasiticide in aquaculture and fisheries. The release of these dyes in aquatic environment without any treatment hinders the development of aquatic animals and plants by blocking out sunlight penetration, being urgent to remove them, especially using bio-friendly methods.

The choice of these two dyes was based on their different molecular sizes and structure but also on their chemical properties. In fact, MO-1 is an anionic type of molecule and GM is a cationic molecule. So, the aim of this work was to understand the interactions between the two distinctive dyes and the biochar samples prepared and modified under different conditions.

The adsorption capacity of the biochar materials was quantified using the Langmuir and Freundlich adsorption models and the results were compared with data obtained previously with a commercial activated carbon.

Experimental

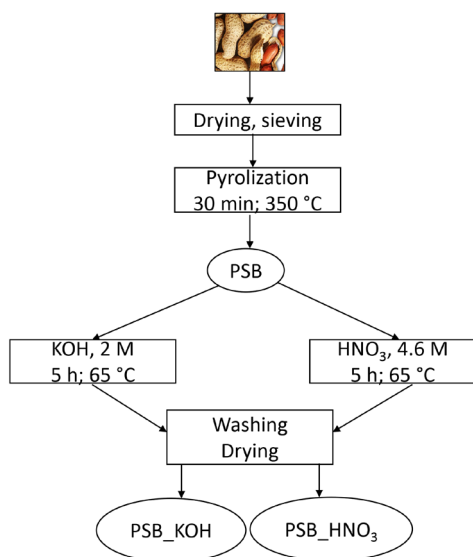
Raw materials and dyes

Peanut shells were obtained from different commercial establishments in Lisbon region to ensure a real waste source. The shells were dried in an oven at 60 °C for 24 h to reduce the water content. The dried materials were mechanically crushed using a mill and separated by sieving in different sizes. The fraction 1000-1400 μm was used in this study. Commercial activated carbon obtained from Panreac (Barcelona, Spain) and identified as AC-P was used as reference adsorption material since it had already been characterized in earlier studies (point of zero charge (pH_{PZC}) = 6.7 and specific surface area (S_{BET}) = 730 m² g⁻¹).²⁵

Both dyes were acquired from Sigma-Aldrich (St. Louis, USA) and were used as received.

Biochar preparation

The biochar was prepared by an oxygen limited pyrolysis method in a muffle furnace. Briefly, around 20 g of the sieved fraction was placed in ceramic capsules and pyrolyzed in a muffle furnace (Thermo Scientific Heareus M110, Waltham, USA) at 350 °C for 30 min. The obtained biochar was labeled PSB (peanut shell biochar). PSB was further treated using alkaline or acid solutions. The alkaline treatment was conducted following the procedure described by Huang *et al.*⁷ Briefly, 10 g of biochar were suspended in 100 mL of 2 M KOH (Sigma-Aldrich, St. Louis, USA), stirred for 5 h at 65 °C using a heating plate with temperature control (IKA C-MAG HS7, Staufen, Germany). Then, the biochar was washed around 10 times using 500 mL of warm deionized water (50 °C) until neutral pH was reached. The powders were recovered by centrifugation (Hermle Z206 A, Wehingen, Germany) and dried at 60 °C overnight. The acid treatment was performed by an analogous procedure but using a 4.6 M HNO₃ solution (Sigma-Aldrich, St. Louis, USA). The modified materials are labeled as PSB-KOH and PSB-HNO₃ for alkaline and acid modified biochars, respectively. Scheme 1 shows schematically the preparation steps performed on peanut shells to obtain the modified biochars.



Scheme 1. Preparation steps of peanut shell based biochars, from pyrolyzation to basic or acid treated samples.

Characterization of biochars

The chemical composition of biochars (carbon, C;

hydrogen, H; and nitrogen, N) was determined in an elemental analyzer (Thermo Scientific Fisons-EA1108 CHNS-O, Waltham, USA) performed at Laboratório Análises, IST, Portugal. The oxygen (O) content was quantified based on mass difference, attending to the contents of C, H and O and the ash content that was quantified by heating the samples at 750 °C for 6 h. The textural properties of base and modified biochars were studied by performing N₂ adsorption isotherms at −196 °C using a tailor-made volumetric apparatus with an assemble of two vacuum pumps: a rotary (RV5) and a diffusion (diffstak MK2) from Edwards (Burgess Hill, UK). The apparatus is made of a customized glass vacuum line lubricated and vacuum sealed taps (Springham) equipped with two pressure sensors (Barocel 600 AB) and Penning (AIM-S-NW225) from Edwards (Burgess Hill, UK).

Prior to the adsorption measurements, the samples (about 50 mg) were degassed under primary vacuum at 300 °C for 2 h in a tubular oven (Eurotherm 2416, Worthing, UK). After cooling, the cell containing the sample was immersed in liquid N₂ (−196 °C) and then the admissions of N₂ (gas) were made at successive relative pressures until reaching a relative pressure higher than 0.95. The specific surface area was determined following the Brunauer-Emmet-Teller (BET) model.²⁶

The surface morphology of the materials was observed by scanning electron microscopy (SEM) using a Hitachi S400 microscope (Tokyo, Japan). The surface functional groups of the samples were investigated on a Bruker Tensor 27 FTIR spectrometer (Bruker Corporation, Billerica, MA, USA). The transmittance was measured from 4000 to 500 cm^{−1} using 32 scans *per* sample and a resolution of 4 cm^{−1}.

The pH values in the point of zero charge, pH_{PZC} were determined by adding 10 mL of deionized water (previously boiled for about 1 h to remove CO₂ and then cooled to room temperature) to 0.5 g of biochar sample. The slurries were left under stirring for 24 h and the pH was measured using a glass electrode (Crison, GLP22, Barcelona, Spain).

Adsorption experiments

For the adsorption studies, 50 mg of the biochar samples were accurately weighted and placed in 50 mL stoppered flasks. Then, 40 mL of dye solutions previously prepared with concentration ranging from 2 to 50 mg L^{−1} were added to the flasks and stoppered. The flasks were immersed in a thermostatic bath at 30 °C (Julabo MP, Seelbach, Germany) which is placed on a multiposition magnetic stirrer (Selecta Multimatic 9-S, Barcelona, Spain) for about 2 h, then samples were taken periodically. The biochars were separated from

the dye solution using membrane filters (Milipore Durapore, 0.45 μm HV, Merck, Darmstadt, Germany) and aliquots of each solution were taken and their absorbances were measured in a double beam spectrophotometer (Jasco V530, Tokyo, Japan) using deionized water as reference and standard cell of 10- or 2-mm optical lengths. Prior to the adsorption measurement, a calibration curve was performed at 385 nm using dye solutions with concentration range needed to obtain absorbances comprised between 0.15 and 1.5, to obey Beer-Lambert law. Each data point resulted from an average of at least three individual aliquots/scans assuring a standard deviation below 5%. The amount of each dye q_t (mg g^{-1}) at a certain time, t , was calculated according to equation 1:

$$q_t = \frac{C_0 - C_t}{W} \times V \quad (1)$$

where C_0 and C_t correspond to the initial concentration and the concentration measured after a certain period, respectively, V is the volume of solution, and W is the mass of biochar sample.

The adsorption isotherm equilibrium studies were performed according to the procedure described above. After 2 h of contact between the dye solutions and the biochar samples, the equilibrium is reached between the two phases. This contact time was tested previously to assure that all biochar samples reached equilibrium. The solution pH was adjusted when necessary to assure it maintained its original valor around 7.

As the experimental absorbance values only allow to obtain the concentration of dye that remained in solution, the amount of adsorbed dye, q_e , (mg g^{-1}) is calculated using equation 2:

$$q_e = \frac{C_0 - C_e}{W} \times V \quad (2)$$

where C_e is the equilibrium concentration of the dye (mg L^{-1}).

The relation between the amount of dye adsorbed on the biochar sample and the equilibrium concentration of the dye solution can be described by different models. The Langmuir model is widely used to obtain characteristic parameters of adsorbate-adsorbent interactions in liquid phase, assuming the formation of an adsorbate monolayer at the surface of the adsorbent material.^{27,28} The model can be mathematically described by equation 3:

$$q_e = \frac{q_m \times K_L \times C_e}{1 + K_L \times C_e} \quad (3)$$

where q_m is the adsorption capacity (mg g^{-1}), K_L is the Langmuir constant (L mg^{-1}), which can be related with the affinity between the adsorbent and the adsorbate.

When the distribution of active adsorption sites on the adsorbent surface is heterogeneous the Freundlich model can also be used, equation 4:

$$q_e = K_F \cdot C_e^{1/n} \quad (4)$$

where K_F is the adsorption coefficient (L mg^{-1}); n is the coefficient of the Freundlich model.

These parameters of both models can be calculated using a nonlinear regression minimizing the errors using the least square's method.

Results and Discussion

Characterization of biochars

The properties of the biochar samples produced in this study are summarized in Table 1.

The PSB yield is relatively higher when compared with values taken from literature⁶ that is commonly around or below 50%, depending on the source of biomass and the experimental parameters used during the pyrolysis. Siddiqui *et al.*²⁹ showed the effect of several parameters: particle size, temperature and time of pyrolysis using waste pomegranate peel and showed that the highest yields are obtained for low pyrolysis temperature, short times and large particle sizes. In this case, the low temperatures, 350 °C, short heating period (30 min) associated with 1000 to 1400 μm particle size and the nature of the biomass source can justify the high yields of PSB. Regarding the treated biochars, the effect of KOH treatment on PSB-KOH yields was mild, whereas for PSB-HNO₃ the effect is much more severe. In the elemental analysis, the O quantification was calculated by subtracting from the total mass the ash, C, H and N contents. As can be observed, the amount of oxygen increased for the treated samples, especially for PSB-HNO₃, as also noted for the O/C ratio. There is also a significant increase on the amount of nitrogen for PSB-HNO₃ sample, which can be ascribed to the formation of nitro groups.³⁰ The pH_{PZC} values taken for PSB samples are like the ones obtained for commercial carbons, i.e., close to neutrality. Upon the treatments with KOH or HNO₃, the pH_{PZC} changes significantly to basic or acid, respectively, denoting the changes of the surface chemistry as a consequence of the basic or acid treatment performed on the materials.

The textural properties of biochar samples were studied through low temperature N₂ adsorption isotherms

Table 1. Characterization of biochar samples: yield, elemental analysis, pH_{PZC} , S_{BET}

Sample	Yield ^a / %	Elemental analysis / wt.%				Atomic ratio O/C	Ash / %	pH_{PZC}	S_{BET} / (m ² g ⁻¹)
		C	H	N	O ^b				
PSB	78	61.4	2.0	1.7	29.6	0.48	5.3	6.2	18.1
PSB-KOH	73 (94)	50.0	2.5	1.2	31.5	0.63	14.8	9.1	20.9
PSB-HNO ₃	48 (62)	54.4	2.0	3.2	40.3	0.74	0.1	3.3	25.9

^aYield values taking raw peanut shells as reference. The yield values taking PSB as reference are indicated in brackets. ^bOxygen content was estimated as follows: $\text{O} = 100\% - (\text{C}\% + \text{H}\% + \text{N}\% + \text{ash}\%)$. pH_{PZC} : point of zero charge; S_{BET} : specific surface area; PSB: peanut shell biochar.

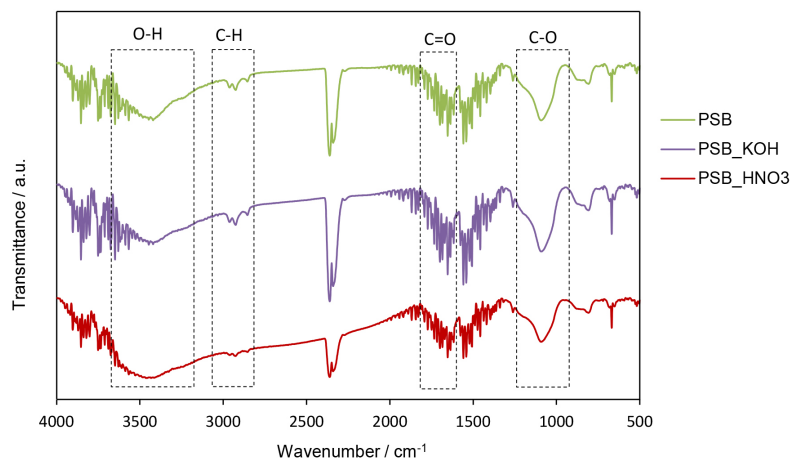
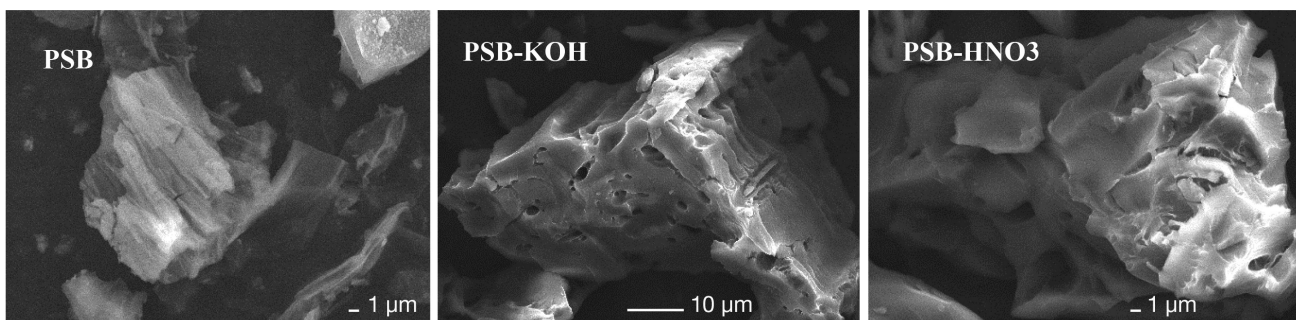
performed at $-196\text{ }^{\circ}\text{C}$. The adsorption isotherms present the same configuration for all samples (not shown) that corresponds to type I + type IV.²⁶ Table 1 shows the values obtained for the S_{BET} . As observed, there is an increase of S_{BET} for the modified biochar samples, as expected, especially for PSB-HNO₃, which is probably related to the higher amount of oxygen functional groups, corroborated by the higher content of oxygen quantified in the elemental analysis. This fact is also in part confirmed by the Fourier transform infrared (FTIR) analysis of the tested samples (Figure 2). All the samples show similar bands from carbon and oxygen functional groups as expected from biomass derivatives, namely the C–O stretching ($1200\text{--}1080\text{ cm}^{-1}$), C=O stretching ($1680\text{--}1620\text{ cm}^{-1}$), C–H stretching ($2980\text{--}2900\text{ cm}^{-1}$).³¹ However, the band from O–H stretching

($3500\text{--}3400\text{ cm}^{-1}$) is more intense in the case of the PSB-HNO₃ sample.

On the other hand, when confronting the textural data with SEM images taken for parent PSB and treated samples displayed in Figure 3, it can be noted that some corrosion/degradation of the particle is more noticeable for the treated samples, especially for PSB-HNO₃, also in line with the values presented for S_{BET} .

Adsorption essays

In all cases, the time needed to reach the equilibrium between the dye solutions and the biochar samples was about 2 h. Therefore, the equilibrium time found was further used to perform the isotherm studies.

**Figure 2.** FTIR (KBr) spectra for PSB, PSB-KOH and PSB-HNO₃.**Figure 3.** SEM images of parent PSB and treated samples.

The non-linear fitting results of the adsorption isotherms for the two dyes are shown in Figure 4 for the parent PSB and for the two modified biochars. The adsorption parameters obtained upon the application of the Langmuir and Freundlich adsorption isotherms are displayed in Table 2. The non-linear regression analysis and statistical parameters were estimated using TableCurve 2D[®],³² and in all cases, the statistical parameters show a good agreement between the experimental data and the two isotherm models. However, a closer inspection of the statistical parameters reveals a better fitting of the experimental data to the

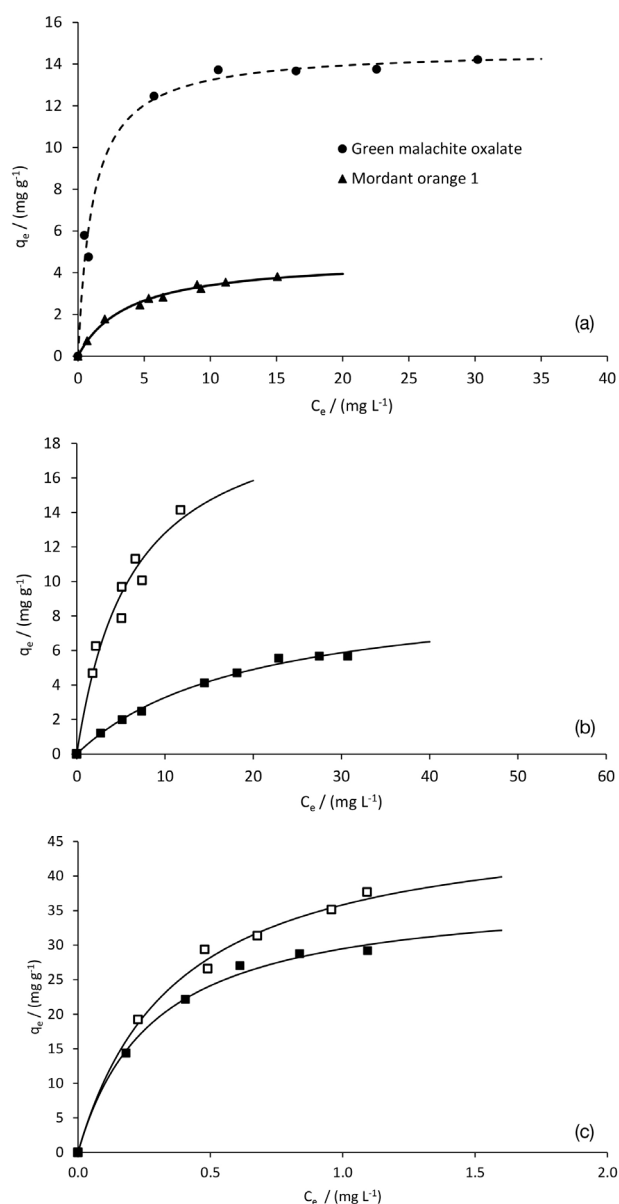


Figure 4. Equilibrium adsorption isotherms of Mordant Orange 1 and Green Malachite oxalate in the parent PSB sample (a), Mordant Orange 1 (b) and Green Malachite oxalate (c) for PSB-HNO₃ (open symbol) and PSB-KOH (close symbol) samples. 30 °C, V = 40 mL, m ca. 0.05 g and pH ca. 7.

Langmuir model, indicating that the adsorption process follows the assumptions of this model, i.e., the formation of an adsorbate monolayer at the surface of the adsorbent materials.²⁷ This information is corroborated additionally by the values of n in the Freundlich isotherm model higher than one indicative of normal Langmuir isotherm.

The analysis of the adsorption models in the parent biochar, PSB, and in both treated samples, PSB-KOH and PSB-HNO₃, shows a significant lower adsorption capacity, q_m , when compared with a commercial activated carbon, AC-P, in both dyes. This behavior was expected due to the much higher surface area of AC-P sample, 730 m² g⁻¹,²⁵ when compared to the values displayed in Table 1. However, a direct comparison based on the adsorption capacity should also consider the higher cost involved in the production of activated carbons when compared with the valorization of peanut shell residues with low production costs due to mild temperatures used during the pyrolysis process. Additionally, as can be observed from the data in Table 2, upon simple basic or acid treatments, the adsorption capacity can increase substantially. Table 3 confronts the results obtained in this study with the literature concerning the removal of several dyes using biochar materials obtained from peanut shells.

As can be observed, the q_m values for the materials prepared in the present study are within the same range, or even higher, when compared with the samples prepared under milder conditions.

To unravel the factors that influence the adsorption capacity, the effects both on the adsorbent and also on the dye must be analyzed.

As shown before, one of the outcomes of the treatments was the increase of surface area. As such, we correlated the Langmuir adsorption capacity and the specific surface area, depicted in Figure 5. The correlation suggests that the small increase in the surface area probably promotes access of the dye molecules to a higher number of surface functional groups on the biochar (Figure 6).

When comparing the results obtained for the two dyes, it is apparent that the differences between them cannot be simply explained by the adsorption capacity of the biochars. In fact, it can be observed that the parent PSB material shows an adsorption capacity of MG about 3 times higher (Langmuir model) when compared with the adsorption of MO-1 on the same sample.

This behavior can be explained based on two phenomena already observed by other authors.^{11,36} One is the higher number of electrons of the three aromatic rings on the MG dye that can establish nonspecific interactions with the carbon surface groups (hydrophobic effects, Figure 6).

Table 2. Langmuir and Freundlich isotherm parameters with the fitting statistical parameters

Dye	Parameter	Adsorbent			
		AC-P	PSB	PSB-KOH	PSB-HNO3
Mordant Orange 1 (MO-1)	$q_m / (\text{mg g}^{-1})$	299.2 ± 6.8	4.7 ± 0.2	9.7 ± 0.6	20.8 ± 3.4
	$K_L / (\text{L mg}^{-1})$	2.5 ± 0.6	0.26 ± 0.03	0.051 ± 0.007	0.16 ± 0.05
	R^2	0.988	0.994	0.994	0.961
	R^2_{adj}	0.983	0.992	0.993	0.947
	FSE	11.927	0.104	0.169	0.922
Langmuir isotherm					
Green Malachite oxalate (MG)	$q_m / (\text{mg g}^{-1})$	321.0 ± 5.1	14.7 ± 0.5	37.9 ± 1.6	49.1 ± 2.6
	$K_L / (\text{L mg}^{-1})$	4.2 ± 0.5	0.9 ± 0.2	3.5 ± 0.5	2.7 ± 0.4
	R^2	0.995	0.980	0.996	0.993
	R^2_{adj}	0.992	0.973	0.993	0.991
	FSE	9.757	0.826	0.783	1.109
Mordant Orange 1 (MO-1)	$K_F / (\text{mg g}^{-1})$	231.7 ± 9.1	1.2 ± 0.1	0.8 ± 0.1	3.7 ± 0.5
	n	11.4 ± 2.2	2.3 ± 0.2	1.7 ± 0.1	1.8 ± 0.2
	R^2	0.989	0.983	0.984	0.970
	R^2_{adj}	0.985	0.978	0.979	0.959
	FSE	11.359	0.173	0.283	0.811
Freundlich isotherm					
Green Malachite oxalate (MG)	$K_F / (\text{mg g}^{-1})$	218.2 ± 21.7	7.1 ± 0.9	29.9 ± 1.1	36.4 ± 0.7
	n	8.3 ± 2.3	4.4 ± 0.8	2.7 ± 0.4	2.5 ± 0.2
	R^2	0.960	0.942	0.983	0.992
	R^2_{adj}	0.934	0.919	0.972	0.989
	FSE	29.503	1.421	1.637	1.179

q_m , K_L : Langmuir isotherm parameters; K_F , n: Freundlich isotherm parameters; R^2 : coefficient determination; R^2_{adj} : adjusted coefficient determination; FSE: fit standard error; PSB: peanut shell biochar.

Table 3. Comparison of the adsorption capacity (q_m) in several dye removal treatments for the peanut shell-based adsorbents prepared in this study and other found on the cited references, modified under the described conditions

Treatment	Dye	$q_m / (\text{mg g}^{-1})$
Washed, dried, powdered, sieved and activated with NaOH at 145 °C for 8 h ³³	Remazol Orange RGB	15.43
Washed, dried at 110 °C, grinded and sieved (2 mm), activation with H ₃ PO ₄ (1:1.5) at 650 °C for 2 h under N ₂ , soaked in 1% of NaHCO ₃ and washed, dried and sieved < 0.5 mm ³⁴	Direct Blue-86	21.60
Washed, dried at 100 °C for 12 h, crushed and sieved, pyrolyzed at 800 °C for 5 h ¹²	Direct Black 38	141.3
	Reactive Red 141	307.5
Washed, sieved (0.75 mm), impregnation with KOH for 24 h, heating at 800 °C for 2 h under N ₂ , washing with HCl until pH neutral ¹⁹	Methylene Blue	204.08
Dried, sieved (0.8-1.6 mm), mixed with H ₃ PO ₄ (88%) using a ratio peanut-shell:acid = 1:1.5), heating at 650 °C under N ₂ for 2 h, soaked with NaHCO ₃ to neutralize excess acid ³⁵	Acid Yellow 36	66.7
Impregnation with H ₃ PO ₄ (10%) during 24 h, followed by drying at 75 °C for 72 h, pyrolysis at 450 °C for 1.5 h ²⁴	Yellow 11	5.59
This study	PSB-KOH	9.7
	PSB-HNO3	20.8
This study	PSB-KOH	37.9
	PSB-HNO3	49.1

PSB: peanut shell biochar.

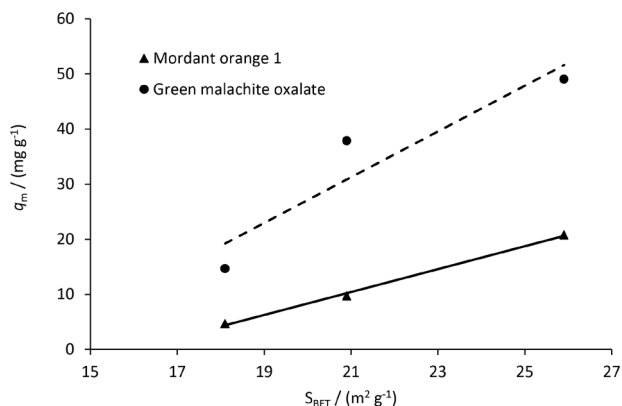


Figure 5. Correlation between Langmuir adsorption capacity, q_m and specific surface area, S_{BET} .

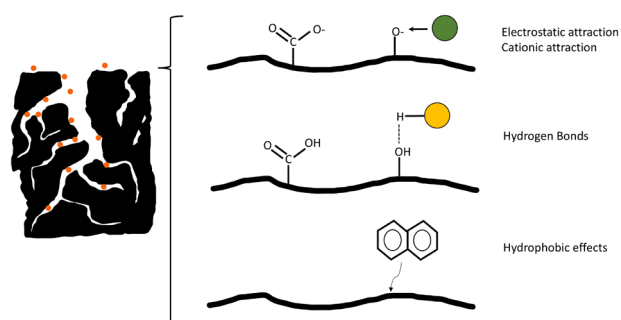


Figure 6. Major adsorption mechanisms in the studied biochars.

The other phenomena that can explain the increase adsorption capacity of some of the treated samples are related with the pH of the dye solutions and the pH_{PZC} of the adsorbent materials.^{11,37} Considering that the pH of the dye solutions was kept around 7 during the experiments and that the pH_{PZC} is around 6 for PSB and 3.3 for PSB-HNO₃ (see Table 1), the pH_{PZC} is lower than the pH of the dye solutions, which will cause an excess of negative charge at the surface of the adsorbent materials. Taking into account the pK_a values and the equilibrium time for the GM at pH 7, the prevalent form should be the cationic dye salt over the carbinol base.³⁸ So, higher adsorption capacity can be explained by the electrostatic attraction between the cationic dye and the negative charged biochars, (electrostatic attraction, Figure 6) especially for PSB-HNO₃ where the difference between pH and pH_{PZC} is more substantial.

In the case of the MO-1, the electrostatic attractions are not relevant since at pH 7 it is totally in the acid form, however it still can occur hydrogen bonds between the dye –OH and –COOH groups and the biochar surface oxygen functional groups (hydrogen bonds, Figure 6).

Conclusions

The results of this study show that it is possible to produce low-cost biochars using food wastes as raw

materials, in this case, peanut shells. The properties of these adsorbent materials can be optimized through simple acid or basic treatments that modify the texture and pH_{PZC} of the adsorbents. Equally important as the specific surface area of the materials, the combination of the pH of the dye solutions with the pH_{PZC} of the adsorbent materials is a factor that should be designed according to the nature of the molecules that are planned to be removed to maximize the adsorption capacity.

Acknowledgments

The authors wish to acknowledge Inês Felicíssimo from EPS for carrying out the adsorption experiments. Financial support for this work was provided by Fundação para a Ciência e Tecnologia through UIDB/00100/2020, UIDP/00100/2020 and LA/P/0056/2020.

References

- Katheresan, V.; Kansedo, J.; Lau, S. Y.; *J. Environ. Chem. Eng.* **2018**, *6*, 4676. [Crossref]
- Nigam, P.; Armour, G.; Banat, I. M.; Singh, D.; Marchant, R.; *Bioresour. Technol.* **2000**, *72*, 219. [Crossref]
- Tiwari, D. P.; Singh, S. K.; Sharma, N.; *Appl. Water Sci.* **2015**, *5*, 81. [Crossref]
- Hu, Q. H.; Qiao, S. Z.; Haghseresht, F.; Wilson, M. A.; Lu, G. Q.; *Ind. Eng. Chem. Res.* **2006**, *45*, 733. [Crossref]
- Rodríguez-reinoso, F.; *Carbon* **1998**, *36*, 159. [Crossref]
- Tripathi, M.; Sahu, J. N.; Ganesan, P.; *Renewable Sustainable Energy Rev.* **2016**, *55*, 467. [Crossref]
- Huang, H.; Tang, J.; Gao, K.; He, R.; Zhao, H.; Werner, D.; *RSC Adv.* **2017**, *7*, 14640. [Crossref]
- Monisha, R. S.; Mani, R. L.; Sivaprakash, B.; Rajamohan, N.; Vo, D.-V. N.; *Environ. Chem. Lett.* **2022**, *20*, 681. [Crossref]
- Praveen, S.; Jegan, J.; Bhagavathi Pushpa, T.; Gokulan, R.; Bulgariu, L.; *Biochar* **2022**, *4*, 10. [Crossref]
- Malik, R.; Ramteke, D. S.; Wate, S. R.; *Waste Manage.* **2007**, *27*, 1129. [Crossref]
- Franca, A. S.; Oliveira, L. S.; Nunes, A. A.; *Clean: Soil, Air, Water* **2010**, *38*, 843. [Crossref]
- Georgin, J.; Dotto, G. L.; Mazutti, M. A.; Foletto, E. L.; *J. Environ. Chem. Eng.* **2016**, *4*, 266. [Crossref]
- Wu, J.; Yang, J.; Feng, P.; Huang, G.; Xu, C.; Lin, B.; *Chemosphere* **2020**, *246*, 125734. [Crossref]
- Jung, C.; Park, J.; Lim, K. H.; Park, S.; Heo, J.; Her, N.; Oh, J.; Yun, S.; Yoon, Y.; *J. Hazard. Mater.* **2013**, *263*, 702. [Crossref]
- Jose, S.; Roy, R.; Phukan, A. R.; Shakyawar, D. B.; Sankaran, A.; *Clean Technol. Environ. Policy* **2022**, *24*, 1599. [Crossref]
- Park, M. H.; Jeong, S.; Kim, J. Y.; *J. Environ. Chem. Eng.* **2019**, *7*, 103039. [Crossref]

17. Sun, K.; Tang, J.; Gong, Y.; Zhang, H.; *Environ. Sci. Pollut. Res.* **2015**, *22*, 16640. [Crossref]
18. Ye, Q.; Li, Q.; Li, X.; *Environ. Pollut. Bioavailability* **2022**, *34*, 385. [Crossref]
19. Han, X.; Chu, L.; Liu, S.; Chen, T.; Ding, C.; Yan, J.; Cui, L.; Quan, G.; *BioResources* **2015**, *10*, 2836. [Crossref]
20. Gong, R.; Li, M.; Yang, C.; Sun, Y.; Chen, J.; *J. Hazard. Mater.* **2005**, *121*, 247. [Crossref]
21. Ibrahim, I.; Tsubota, T.; Hassan, M. A.; Andou, Y.; *Processes* **2021**, *9*, 149. [Crossref]
22. Yakout, S. M.; Daifullah, A. E. H. M.; El-Reefy, S. A.; *Environ. Eng. Manage. J.* **2015**, *14*, 473. [Crossref]
23. Liu, L.; Li, Y.; Fan, S.; *Processes* **2019**, *7*, 891. [Crossref]
24. Kouadio, D. L.; Diarra, M.; Tra, B. T. D.; Akesse, D. P. V.; Soro, B. D.; Aboua, K. N.; Meite, L.; Kone, M.; Dembele, A.; Traore, K. S.; *Int. J. Innov. Appl. Stud.* **2019**, *26*, 1280. [Crossref]
25. Martins, A.; Nunes, N.; *J. Chem. Educ.* **2015**, *92*, 143. [Crossref]
26. Gregg, S. J.; Sing, K. S. W.; *Adsorption, Surface Area, and Porosity*, 2nd ed.; Academic Press: London, 1995.
27. Langmuir, I.; *J. Am. Chem. Soc.* **1918**, *40*, 1361. [Crossref]
28. Moreno-Castilla, C.; *Carbon* **2004**, *42*, 83. [Crossref]
29. Siddiqui, M. T. H.; Nizamuddin, S.; Mubarak, N. M.; Shirin, K.; Aijaz, M.; Hussain, M.; Baloch, H. A.; *Waste Biomass Valorization* **2019**, *10*, 521. [Crossref]
30. Stavropoulos, G. G.; Samaras, P.; Sakellariopoulos, G. P.; *J. Hazard. Mater.* **2008**, *151*, 414. [Crossref]
31. Pandey, S. D.; Mendonça, F. G.; Rodrigues, M. N.; Faria, B. P. Z.; Campos, J. L. E.; Noronha, I. F. P. C.; Vieira, S. S.; Santos, N. A. V.; Fernandes, L. A.; Sampaio, R. A.; Colen, F.; Magriotis, Z. M.; Jorio, A.; *J. Environ. Manage.* **2021**, *279*, 111685. [Crossref]
32. *TableCurve 2D*, version 5.01; Systat Software Inc., Chicago, USA, 2002.
33. Acemioğlu, B.; *Int. J. Coal Prep. Util.* **2022**, *42*, 671. [Crossref]
34. Garg, D.; Majumder, C. B.; Kumar, S.; Sarkar, B.; *J. Environ. Chem. Eng.* **2019**, *7*, 103365. [Crossref]
35. Garg, D.; Kumar, S.; Sharma, K.; Majumder, C. B.; *Groundwater Sustainable Dev.* **2019**, *8*, 512. [Crossref]
36. Gong, R.; Jin, Y.; Chen, F.; Chen, J.; Liu, Z.; *J. Hazard. Mater.* **2006**, *137*, 865. [Crossref]
37. Wang, X. S.; Zhou, Y.; Jiang, Y.; Sun, C.; *J. Hazard. Mater.* **2008**, *157*, 374. [Crossref]
38. Culp, S. J.; Beland, F. A.; *J. Am. Coll. Toxicol.* **1996**, *15*, 219. [Crossref]

Submitted: August 15, 2022

Published online: December 15, 2022

